SAND--82-1252C
Conf-820944--4

SAND--82-1252C

DE82 021082

MASTER

DIAGNOSING LIGHT-ION-BEAM DIODES*

C. W. Mendel, Jr.
Sandia National Laboratories, Albuquerque, NM 87185 (USA)

This lecture will begin with a discussion of diagnostics in ion-beam diodes. This will include electromagnetic measurements, measurements of the electron cloud, and measurements of anode plasmas. A few minutes will be spent on diagnostics of distributed ion sources required for one class of ion diodes, the plasma-filled versions, which require high-density, highly ionized sources of very uniform plasma. The measurements of the beam characteristics will then be discussed. This will be broken into two regions; the region near the diode where diagnostics are generally extensions of those used in other fields; and the region near focus where new diagnostics have been developed.

*This work was supported by the U. S. Department of Energy under contract DE-AC04-76-DP00789.

DISCLAIMER

In the first lecture the characteristics of ion diodes were described. The primary diode measurements are the diode current, ion current and diode voltage. The currents are measured by magnetic probes at various places on the diode. Usually several are averaged to get the current and are differenced to look at symmetry. Rogovsky belts are not usually used because the pulse transit time along their length is too long and precludes a high frequency response. The magnetic probe generally works quite well as long as high current density ion or electron beams do not hit it.

Voltage is another matter entirely. In small experiments the voltage can be measured on the water side of a vacuum interface or in a magnetically insulated line (voltage can be calculated from magnetic measurements) and corrected for inductance between the point where the voltage was measured and the diode. In a large system such as PBFA I this is not possible at present due to the large number of power sources involved (36 for PBFA I). The diode voltage is inferred from the time-dependent ion energy spectrum. The measurement can be done with a time-dependent Thompson parabola,[1] shown schematically in Fig. 2-1. A small spot of proton emitting material (such as nylon mesh) is placed on the positive transmission line near the diode. A portion of the emitted protons pass through a small aperture in the negative line with energy equal to the line voltage times the protonic charge. They then pass through collimating apertures and a region of parallel magnetic and electric field. The magnetic field is constant in time and the electric field rises linearly in time. The deflection normal to the fields is determined by the ratio of magnetic field to momentum (Fig. 2-2). The deflection, therefore, is proportional to one over the square root of voltage. The deflection in the direction of the applied fields is proportional to electric field divided by energy and therefore

to electric field divided by line voltage. Since line voltage is inferred from the measured magnetic deflection, we then know the electric field in the spectrometer corresponding to that line voltage. Since we know electric field as a function of time, we can infer the time at which the voltage occurred. The data is recorded with a channel plate amplifier, phosphor, and film combination. The channel multiplier array output could easily be recorded with a diode array such as those used in digitizing oscilloscopes, thus providing a fast readout straight to a computer.

Although a suitable ion diode for a reactor will not be exactly like the plasma filled version shown earlier, it is likely that they will be plasma filled. This is because they must operate for many pulses without maintenance. Dielectric anodes are essentially destroyed on their first shot. It will be desirable to monitor the plasma fill density continually. In plasma filled diodes you will recall that the plasma is pushed rapidly away from the cathode by the magnetic field of the series coil. Therefore the time-dependent gap between cathode and plasma anode can be measured by measuring field coil voltage (typically 50 kV) integrating it to get flux and dividing by coil current.[2] The coil inductance is proportional to the diode gap X

$$L(X) = L + KX$$

where K is a constant dependent upon the actual coil design. The gap opening velocity is given by[3]

$$dX/dt = b_o/2A\ (\mu_o/n_i m_i)^{1/2}\ I$$

which is related to the Alfven velocity. In this expression n_i is the ion density of the anode plasma, m_i is the ionic mass, A is the diode area, and b_o is a constant with units of length relating the diode current to the magnetic field (recall that the field coil is in series with the diode). Differentiating L(X) with respect to t and taking the ratio of dL/dt to DX/dt we can then get an expression for n_i

$$n_i = (Kb_o/2A)^2 \mu_o/m_i \ (dL/dQ)^{-2}$$

where $I = dQ/dt$ has been used. Figure 2-3 shows data from a plasma filled diode. The plots are L vs Q for four different plasma fill densities. The plasma density from the above expression is shown with each plot. This measurement works quite well but it is of course an average measurement over the anode plasma surface.

Another method of measuring plasma densities in the range needed is the measurement of the collisionless skin depth using microwaves. In the method we have used at Sandia, a wave travels down a waveguide toward a slot in the surface of an electrode at which the measurement is desired. The slot is covered with a thin mylar film so that the waveguide is empty, and the plasma is only on the electrode side of the film (Fig. 2-4). The width of the slot is equal to the standard waveguide width, but the height (in the E field direction) is much smaller than a wavelength. For the 13 mm wavelength data to be presented the slot height was 1 mm. With no plasma over the film the line reflects as an open line. As the electron density increases the phase of the reflected wave shifts until it is 180° out of phase with the zero density reflection at densities such that the skin depth is small compared to the

slot height. The phase shift is readily measured by standard microwave techniques. Figure 2-5 shows a phase plot of some data taken on a laboratory plasma gun. Below critical density there is some radiation from the slot, so the reflected wave is smaller. At high density the collisions attenuate the reflected wave. Figure 2-6 shows the decay of a plasma in an electron diode experiment. The exponential decay is an indication of the quality of the measurement. This diagnostic has been used in our plasma source research and also to measure pre-pulse plasmas caused by low level (~ 10 kV) pulses preceeding the main power pulse in diode experiments. The theory of the measurement can be done analytically because of the small ratio of the slot height to the wavelength of the microwaves. The primary difficulties are that the measurement is close to the surface of an electrode, and that microwave detectors (particularly square-law detectors) have low output voltage. The electro-magnetic pulse around pulsed power machines is typically hundreds of kilovolts per meter so that noise and solid state component damage is a great concern. Thorough electric shielding is essential.

Anode plasmas on dielectric anodes have been measured using spectroscopy and holography.[4,5] The data showed a thin layer of plasma with 5×10^{16} cm^{-3} density and 5 eV temperature, expanding away from the anode at the acoustic velocity. The times of interest are sufficiently long for most holography systems, and the densities are adequate for good sensitivity. The measurements are on diodes specially designed to be accessible and quasi-spherical focusing diodes will be more of a challenge. Since the plasmas on the surface of these anodes are very dense (10^{16} to 10^{18} cm^{-3}) spectroscopic analysis will probably be very useful,[15] but has just begun to be used. These anodes are essentially not understood at all, so this is a valuable place for current research.

The electron cloud in the diode also is very difficult to study. Microwave measurements can be instructive[6,7] and have been discussed earlier at this conference by Chuck Wharton. Time-integrated x-ray photographs of ion diode anodes sometimes show streaked patterns which have been ascribed to electron instability. It does not seem likely that an instability involving electrons alone would be stationary, so there is probably an anode heating mechanism involved in the instability. For electron cloud instability, fast diagnostics are required. Experiments at Cornell[6] have seen microwave bursts followed by x-ray burst in ion diodes. These are believed to be due to electron instabilities driving electrons to the anode resulting in increased bremsstrahlung. Therefore microwave or x-ray bursts can be used to monitor electron cloud instability. Fast x-ray pinhole cameras using depleted U^{238} pinhole apertures and channel multiplier array detectors can be used to photograph the anode x-rays on a one nanosecond time scale. These cameras are now in existence.[8] The primary problem is elimination of the general x-ray background existing near all pulsed power machines. The background has a thick target spectrum extending up to the end point energy corresponding to the machine voltage. The primary problem comes from x-rays of a few tens of kilo-electron volts. Five to ten centimeters of lead with careful attention to avoiding leaks suffices for present machines.

The measurement of the ion beam itself is the most developed area of ion beam fusion diagnostics. The simplest beam diagnostic is the biased charge collector shown in Fig. 7. These are used near the diode at current densities up to a few kA/cm.[2] Since the beam density is typically about 10^{13} cm^{-3} the beam must be neutralized all the way to the collector except for a thin sheath of 0.1 cm thickness where electrons are excluded by the bias voltage. The bias voltage must be

high enough to stop co-flowing electrons, and is typically about - 1 kV. Often the input aperture is covered with a thin foil to stop slower ions. By using several detectors with different thickness foil the voltage waveform can be measured. Some data using this technique can be seen in Fig. 2-8. Notice the sharp onset of current to the detectors as the ion range exceeds the foil thickness (Fig. 2-8b). This technique is simple and is quite reliable. The difficulty for a reactor situation is that the foil would need replacement between successive beam pulses. This could undoubtably be accomplished with moving foil tapes. There has been debate as to the best way to avoid secondary electron problems with these detectors since the beam is a neutral plasma almost all the way to the cup. The simple version shown in the figure seems to compare well with the ion output measured at the diode and also with nuclear measurements to be discussed.

Ions with multi-MeV energies are good candidates for measurements involving nuclear reactions.[8-13] Nuclear diagnostics have been developed at several laboratories, with many of the ideas coming from the Naval Research Laboratory in the United States. The most common and one of the most reliable has been the measurement of proton beams using carbon activation.[9-11] At low current densities (up to about 100 A/cm^2 for 20-30 ns) a small carbon block is placed in the beam. The carbon is activated by the proton beam through the $^{12}C(p,\gamma)^{13}N$ reaction. Immediately after the shot the carbon block is then taken to a coincidence counting detector pair. The ^{13}N decays by emission of a positron through the $^{13}N(\beta^+)^{13}C$ reaction with a 10 min half life. The detector measures the photon pair resulting from the positron annihilation. At higher currents the carbon block ablates and some of the activated carbon is lost. To overcome this the carbon can be placed in a "salt shaker" to contain the ablated material.[10] The salt shaker allows

the beam in through its aperture, but retains most of the ablated carbon inside so its activity is counted. This is satisfactory up to several kA/cm^2. The technique is better suited to single-shot, laboratory experiments than it is to reactor systems, as are all of the activation rections used at present (see Ref. 9 for a list of useful reactions). They have been chosen because they allow sufficient time to get the activated material to the detection system. Reactions with long lifetimes could be used to average the ion output over many pulses, however. Thin foil filters have also been used over carbon activation blocks to increase the energy threshold for detection.

Other nuclear diagnostic, more suited to the reactor environment are the prompt-γ ray diagnostics.[9,11-14] One example is the $^{7}Li(p,\gamma)^{8}Be$ rection shown in Fig. 9. The ion beam impinges on a lithium metal target and reacts with the lithium nuclei. While these reactions have sharp resonances, the thick target yield is broad. This is because all ions more energetic than the resonance pass through it as they slow in the target material. The thick target yield for the reaction is shown in the graph on the figure. Some fraction of the prompt gammas are detected by a scintillator which is well shielded against the extremely intense, but much less energetic bremsstrahlung x-rays from the diode power pulse. A time-integrated measurement can be obtained at the same time by placing a Cu slug near the lithium. The copper is activated by the gammas and then emits positrons. The reaction is $^{63}Cu(\gamma,n)^{62}Cu(\beta^{+})$. The annihillation photon pair can be detected with the same system used for carbon activation. The lithium may ablate in this measurement system without effecting the outcome since the gamma ray appears almost immediately. Lithium salts can replace the metal thereby making handling easier. The prompt gamma measurement with gamma detecting scintillator systems is

well suited to reactor systems. Unwanted neutron signals will arrive well after the gamma pulse, and bremsstrahlung can be shielded out.

An additional measurement of the beam is the divergence. It must be low enough or much of the beam will miss the target in present experiments or the channel in a reactor. The method used for this measurement is to use the ion beam to image an aperture with some figure (a cross in Fig. 2-10) on a heavy metal foil. The foil Rutherford scatters the ions. The image in scattered ions is then imaged on a detector with a pinhole camera. Current devices are quite small (a few cm in each direction) and could be made smaller. The detectors are presently cellulose nitrate plastic[15] which is etched in hot NaOH for several hours. The tracks in the plastic are increased in size by the etching process. A skilled analyst can then tell from the pits how heavy the ion was and can therefore discriminate between different ions. In a reactor the cellulose nitrate would be replaced by a channel electron multiplier array, giving instant readout, but not discriminating between various ion species.

In a reactor system the ion beam will not be focused directly on the target (this is not true for heavy ion fusion or the intermediate ion systems studied by Occidental Petroleum and others).[16,17] It will have to be transported several meters in an ionized channel. These channels must be diagnosed in their own right, and they may also provide an easy way to measure the ion beam. These channels have been studied for several years now.[18-21] The technique which seems to be best suited to ion beam fusion involves heating the target chamber gas (perhaps 100 Torr of argon with small amount of sodium) by a laser pulse tuned to an atomic level of the alkali metal added to the chamber as a dopent. The heated gas drives a

cylinderical shock outward leaving an evacuated cylinder of gas. The low pressure gas in the channel is then ionized by a discharge from a small capacitor bank (Fig. 2-11). Figure 2-12 shows Abel inverted data from several holograms taken at various times during the discharge. These channels are extremely straight and very reproducible. It would be possible to monitor these channels in a reactor by similar diagnostics.

The channels are of high enough density that sophisticated spectroscopic analysis should be valuable. The current density profile would be of great interest. The currents are small enough that Faraday rotation of laser light due to the channel magnetic field on the electrons would give only a small rotation. Zeeman effect on the target chamber gas is a possible diagnostic, however. Using the many techniques developed by Griem[22] and others a great deal of information should be derivable from the spectrum. Since channel diagnosis has barely begun, much opportunity for development remains.

References

1. G. W. Kuswa and P. L. Dreike, private communication.
2. C. W. Mendel, Jr. and G. S. Mills, to be published JAP, Nov. 1982.
3. C. W. Mendel, Jr., P. A. Miller, J. P. Quintenz, D. B. Seidel, and S. A. Slutz, Proc. of the 4th Int'l. Topical Conf. on High-Power Electron and Ion-Beam Research and Technology, Palaiseau, France, June 1981.
4. D. J. Johnson, E. J. T. Burns, J. P. Quintenz, K. W. Bieg, A. V. Farnsworth, Jr., L. P. Mix, and M. A. Palmer, JAP 52, 168 (1981).
5. R. Pal and D. A. Hammer, Cornell Laboratory of Plasma Physics Report No. LPS-302, to be published.
6. Tim Renk and Chuck Wharton, private communication.
7. G. Bekefi, Phys. of Fluids 19, 43 (1976) and Phys. of Fluids 22, 978 (1979).
8. D. L. Fehl, J. Chang, G. W. Kuswa, and C. W. Mendel, Jr., Rev. Sci. Instrum. 51, 2921 (1980).
9. F. C. Young, J. Golden, and C. A. Kapetanakos, Rev. Sci. Instrum 48, 432 (1977).
10. A. E. Blaugrund and S. J. Stephanakis, Rev. Sci. Instrum 49, 866 (1978).
11. F. C. Young. U. S. National Bureau of Standards, publication 628.
12. R. J. Leeper, E. J. T. Burns, D. J. Johnson, and W. M. McMurtry, U. S. National Bureau of Stndards, publication 628.
13. F. C. Young, W. F. Oliphant, S. J. Stephanakis, and A. R. Knudson, IEEE Trans. on Plasma Sci. PS-9, 24 (1981).
14. J. Golden, R. A. Mahaffey, J. A. Pasour, F. C. Young, and C. A. Kapetanakos, Rev. Sci. Instrum. 49, 1384 (1978).
15. C. Hepburn and A. H. Windle, J. of Material Sci. 15, 279 (1980).

16. W. Salisbury and D. Chang, Occidental Research Corp., private communication.
17. Z. G. T. Guiragossian, TRW, private communication.
18. F. L. Sandel, S. J. Stephanakis, F. W. Young, and W. F. Oliphant, Proc. 4th Int'l. Topical Conf. on High-Power Electron and Ion-Beam Research and Technology, Palaiseau France, 1981.
19. J. N. Olsen, JAP 52, 3279 (1981).
20. J. N. Olsen and Louis Baker, JAP 52, 3286 (1981).
21. J. N. Olsen and R. J. Leeper, JAP 53, 3397 (1982).
22. Plasma Spectrocopy, Hans R. Griem (McGraw-Hill, 1964).

Figure Captions

2-1. Swept Thompson parabola for measuring time-dependent ion spectra, from which voltage waveform is determined. The magnetic field is constant and normal to the ion beam. The electric field is parallel to the ion beam and is swept in time.

2-2. The trace of the swept Thompson parabola on the recording medium. At any instant of time the protons must fall on the parabola determined by the electric field at that time. The parabola thus determines time, the deflection determines ion energy and thus line voltage.

2-3. Inductance of the field coil versus charge (integral of diode current) for a plasma filled, series field coil diode (Ampfion). The coil inductance is proportional to diode gap, as is the charge. The slope of the curves are proportional to one over the square root of plasma fill density. The four curves are for four different shots with different plasma fills.

2-4. Diagnostic slot for measuring plasma collisionless skin dept with microwaves. The waveguide is reduced in height by quarter-wave steps. The mylar film keeps plasma out of the waveguide.

2-5. Phase of the wave reflected from the slot for a range of plasma density up to 20 times the critical density (7×10^{12} cm in this case). Below critical density the slot radiates somewhat. This data was taken by stagnating the plasma from a small plasma gun against the plate containing the diagnostic slot.

2-6. Density measured in the after-glow from an electron beam diode. The exponential decay indicates that a good measurement was made over more than two decades in density.

2-7. Biased charge collector. These devices work amazingly well for ion current densities up to a few kA/cm^2. Thin filter foils can be used to eliminate low energy ions, or to use the diagnostic to determine when the voltage reached the level where the output ion range exceeds the foil thickness.

2-8. Measurements of a proton beam (8a). This data agrees well with other methods of measurements. In Fig. 2-8b charge collectors with 8 μm and 16 μm filters show when the proton energy exceeds 0.65 and 1.0 MV.

2-9. Prompt-gamma diagnostic. The protons cause the lithium target to emit gamma-rays through the $Li(p,\gamma)Be$ reaction. These rays are then recorded with scintillators carefully shielded to reduce x-ray background. This diagnostic can give a time-resolved measure of extremely high proton doses.

2-10. Rutherford scattering beam divergence diagnostic. The beam passes through an aperture plate and duplicates the image on a heavy metal scattering foil. Lower beam divergence gives a better quality image. The scattered ion image is then recorded with a pinhole camera and analyzed.

2-11. Experiment to test channel transport of ions. The ion transmission was measured with nuclear diagnostics (50% over 2 m). Holography normal to the channel measured the channel density profile.

2-12. Channel density profiles for four different times as measured by holography and Abel inversion. Error bars are shown at a few representative points.

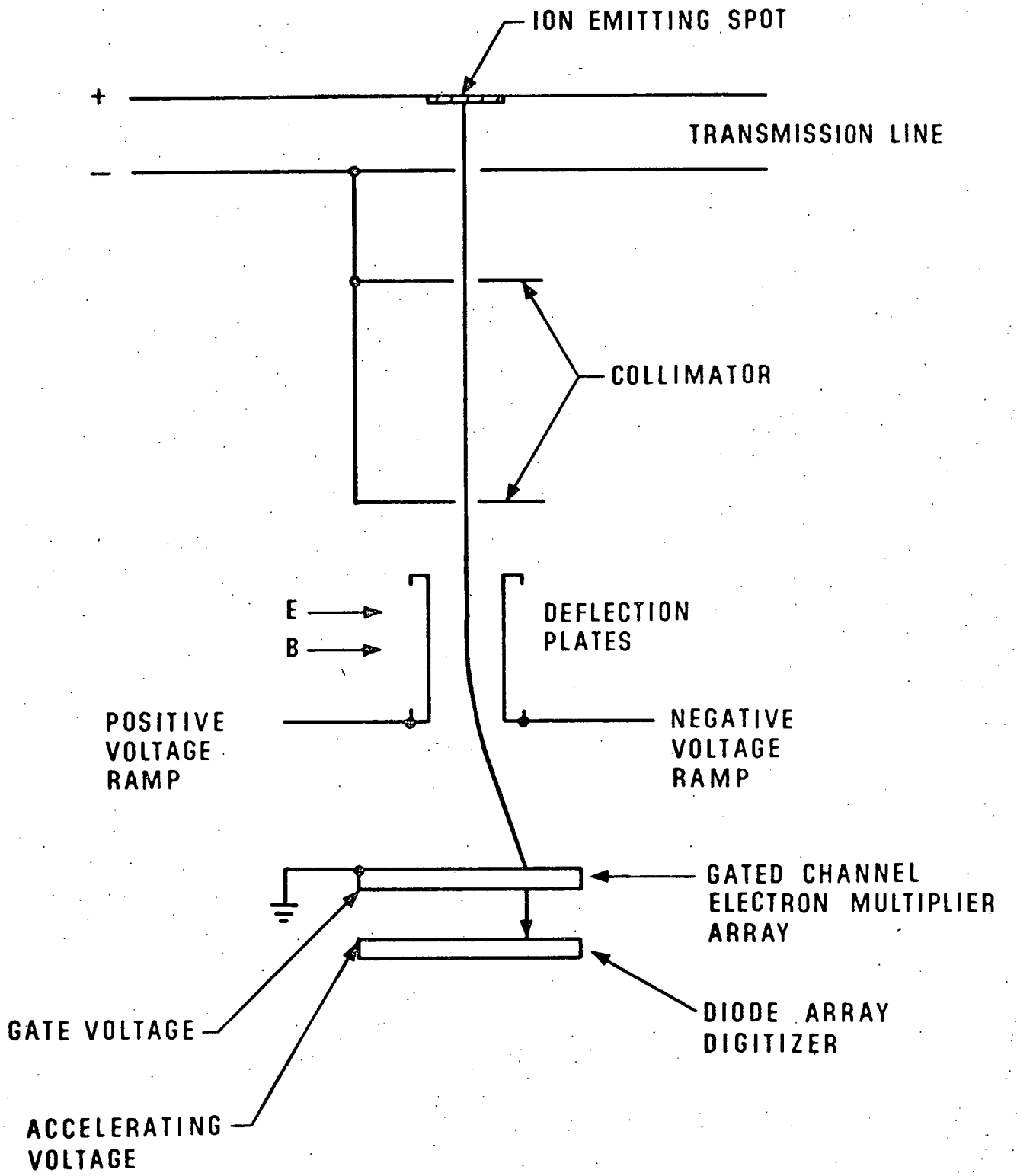
ION EMITTING SPOT
+
TRANSMISSION LINE
−
COLLIMATOR
E
B
DEFLECTION PLATES
POSITIVE VOLTAGE RAMP
NEGATIVE VOLTAGE RAMP
GATED CHANNEL ELECTRON MULTIPLIER ARRAY
GATE VOLTAGE
DIODE ARRAY DIGITIZER
ACCELERATING VOLTAGE

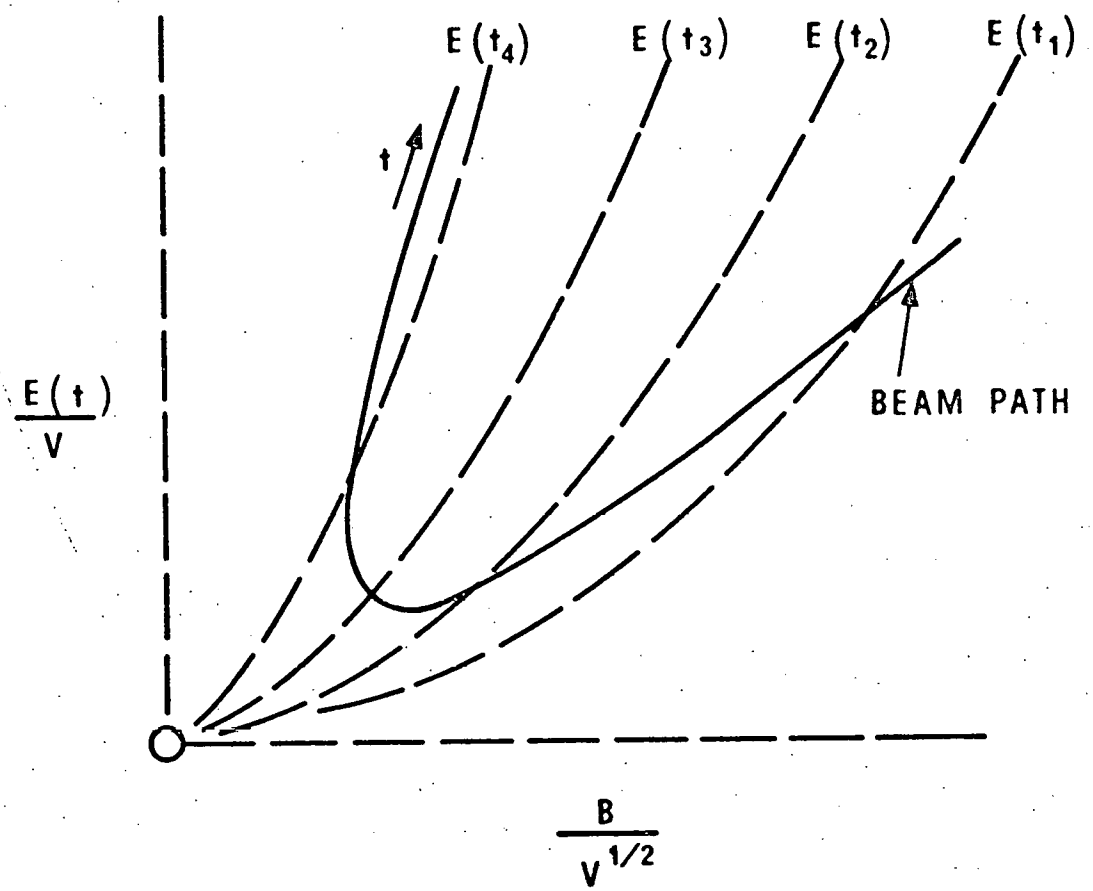
E(t4)
E(t3)
E(t2)
E(t1)
t
E(t)/V
BEAM PATH
B/V^1/2

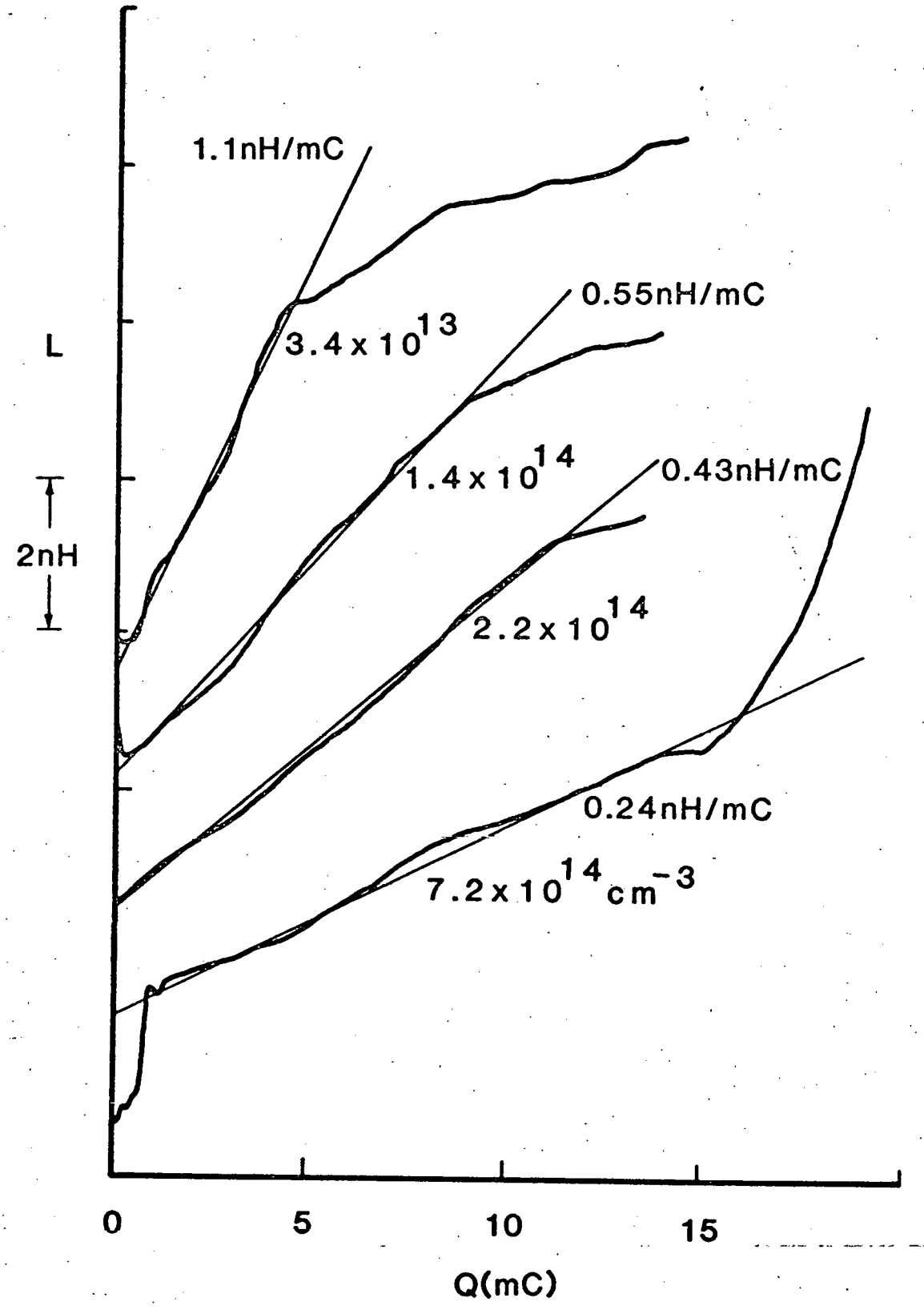
1.1nH/mC
3.4 x 10^13
0.55nH/mC
L
1.4 x 10^14
0.43nH/mC
2nH
2.2 x 10^14
0.24nH/mC
7.2 x 10^14 cm^-3
0
5
10
15
Q(mC)

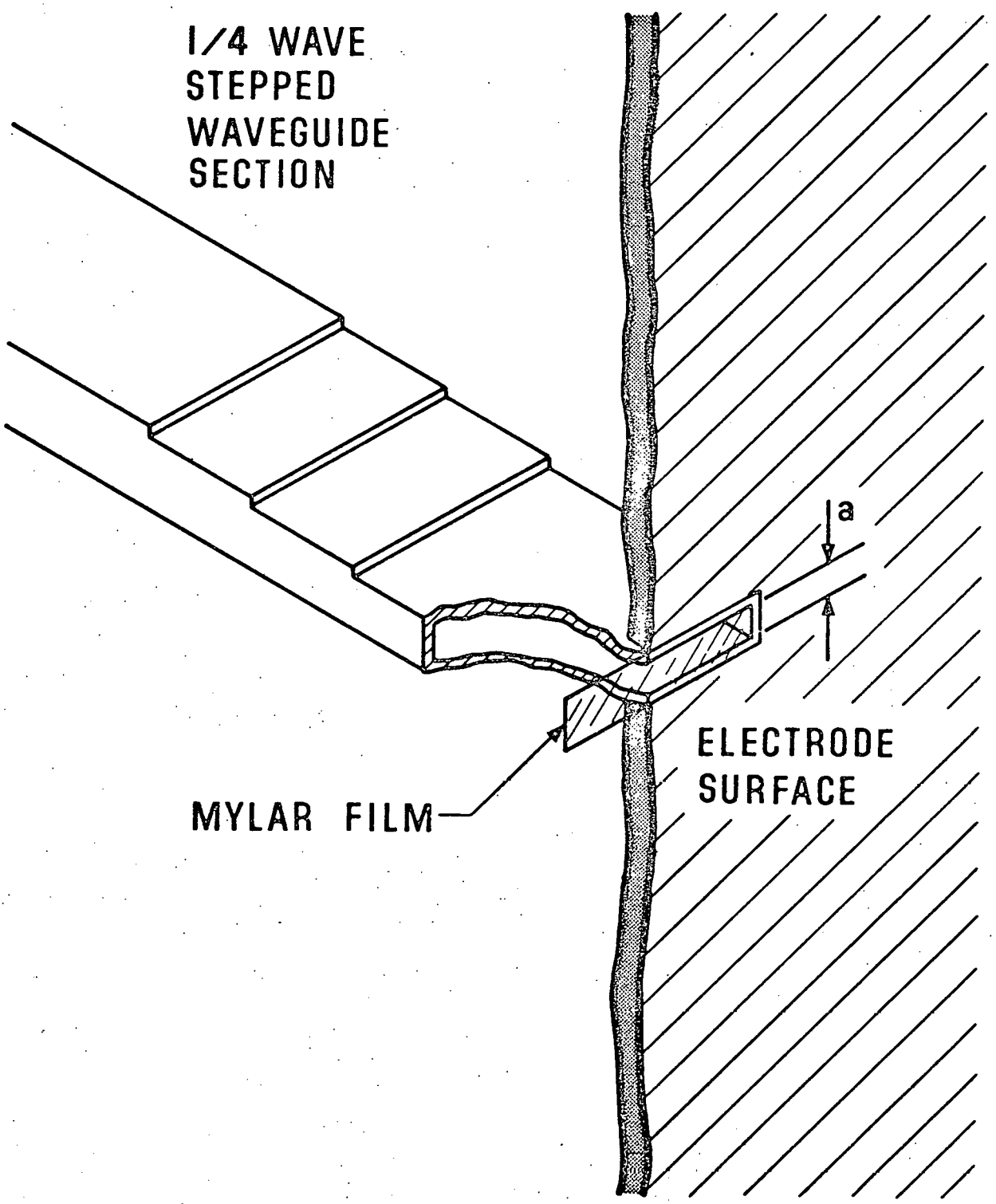
1/4 WAVE
STEPPED
WAVEGUIDE
SECTION
a
ELECTRODE
SURFACE
MYLAR FILM

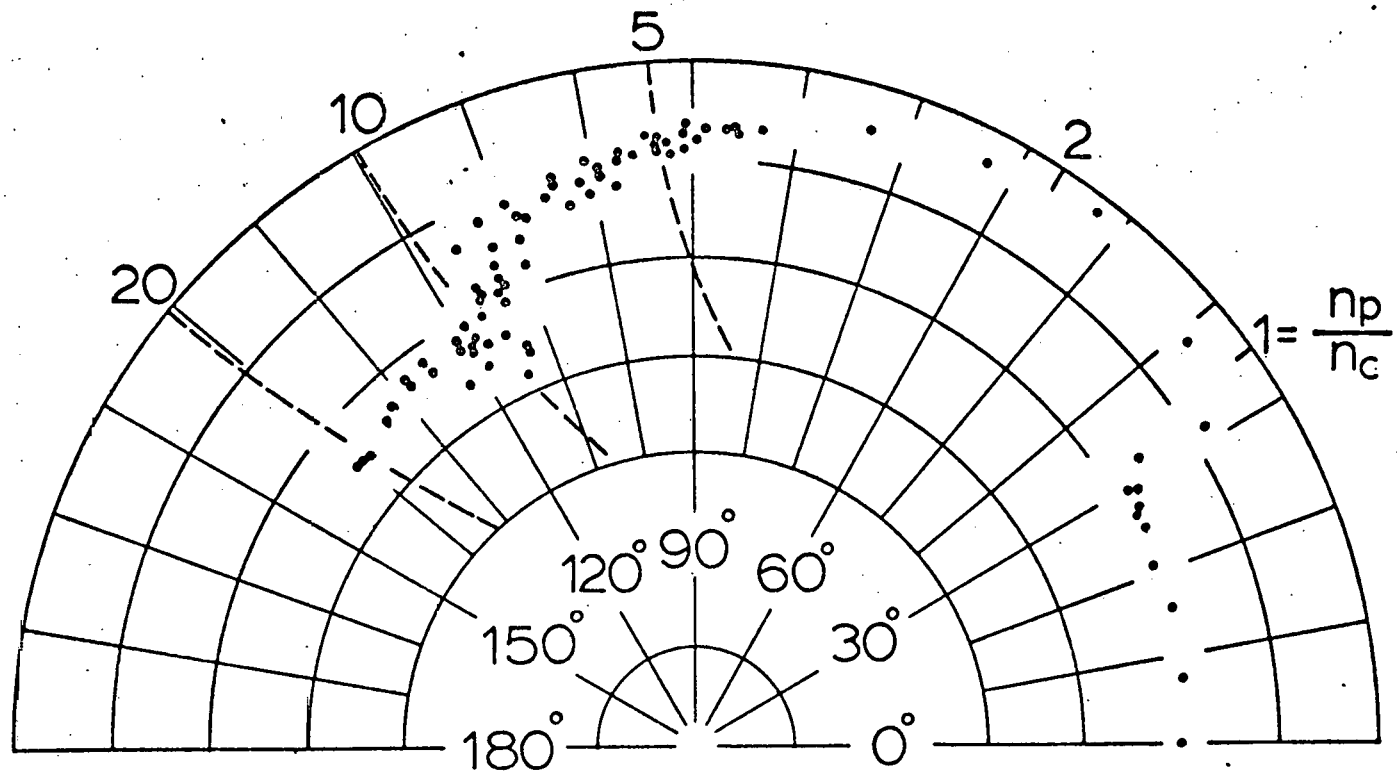
5
10
2
20
1= $\frac{n_p}{n_c}$
120°
90°
60°
150°
30°
180°
0°

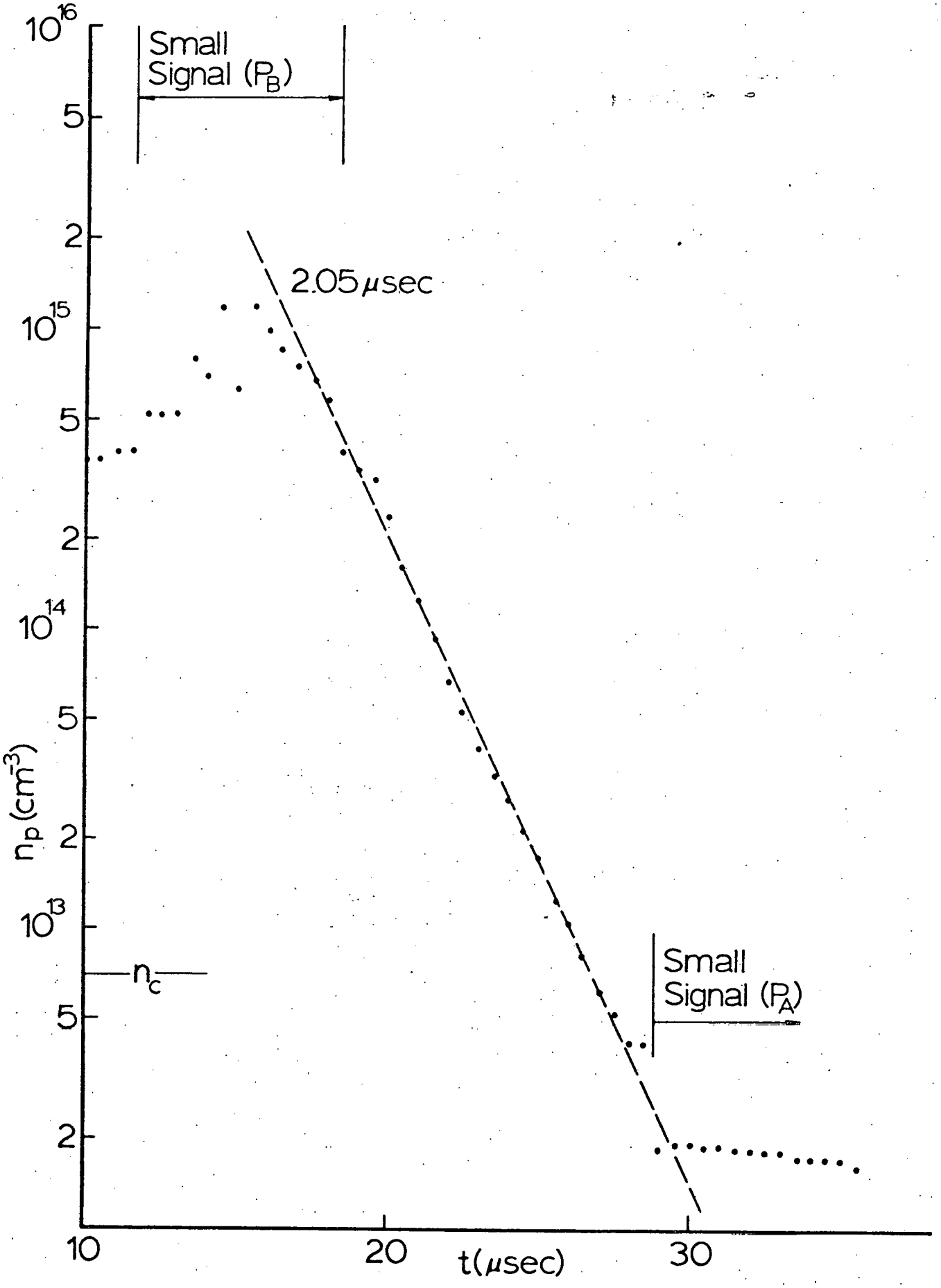
Small
Signal (P_B)
2.05 μsec
Small
Signal (P_A)
n_c
n_p (cm^{-3})
10^{16}
5
2
10^{15}
5
2
10^{14}
5
2
10^{13}
5
2
10
20
30
t(μsec)

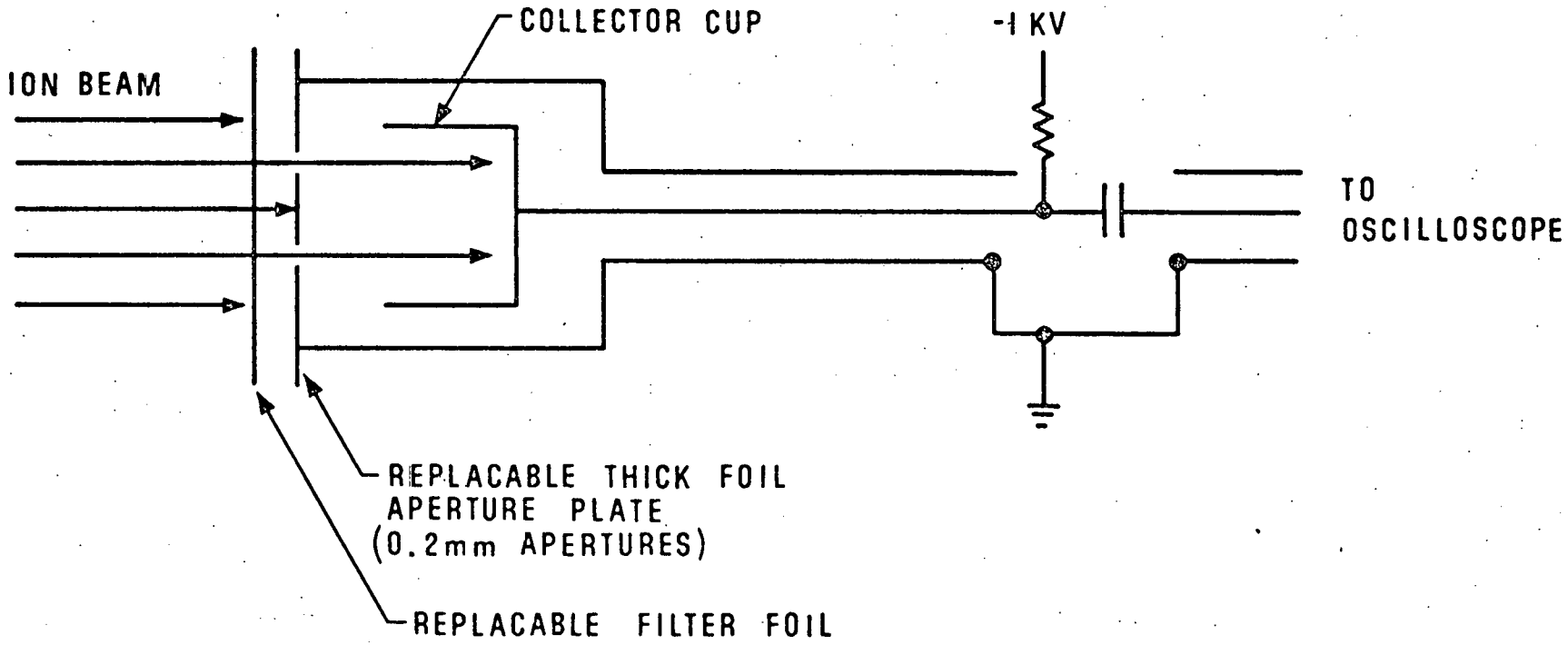
COLLECTOR CUP
-1 KV
ION BEAM
TO
OSCILLOSCOPE
REPLACABLE THICK FOIL
APERTURE PLATE
(0.2mm APERTURES)
REPLACABLE FILTER FOIL

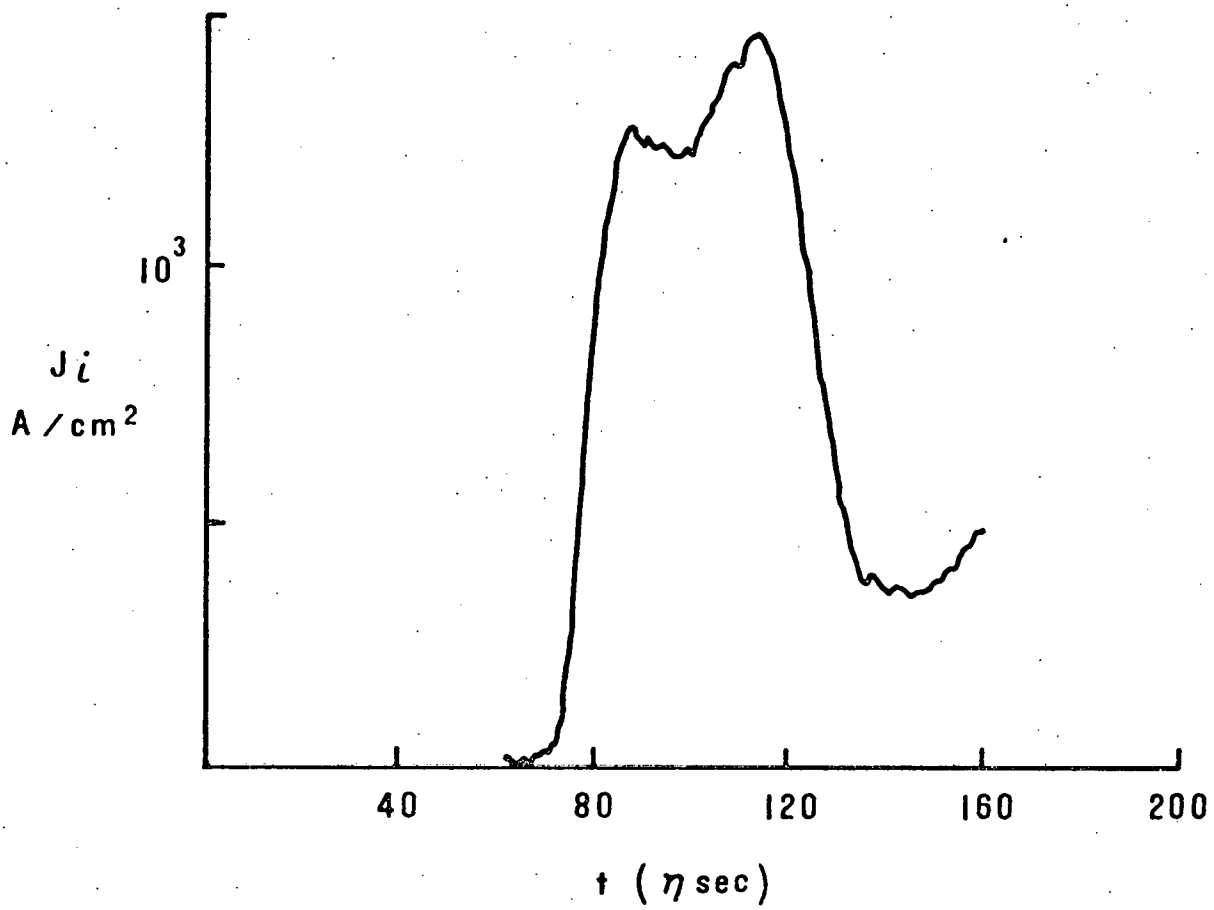
10^3
J_i
A / cm^2
40
80
120
160
200
t (η sec)

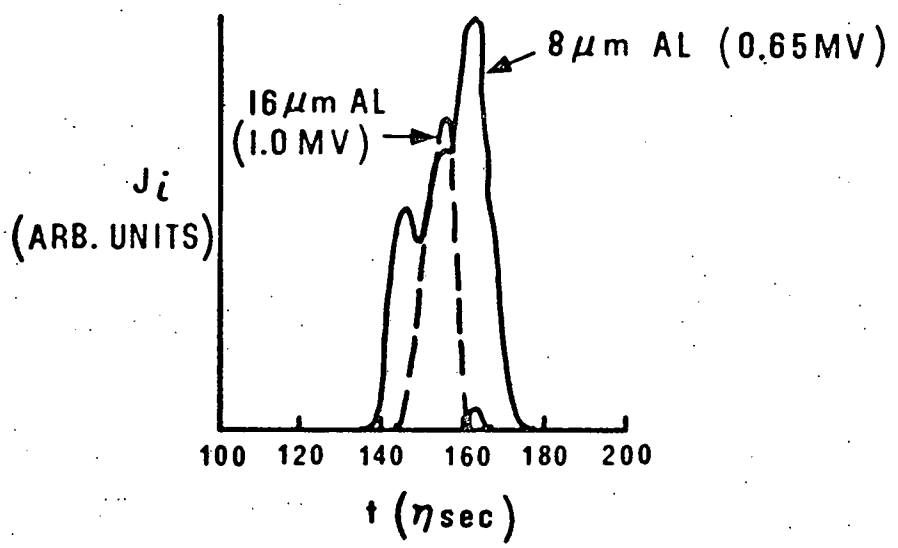
8 μm AL (0.65MV)
16 μm AL
(1.0 MV)
J_i
(ARB. UNITS)
100
120
140
160
180
200
t (ηsec)

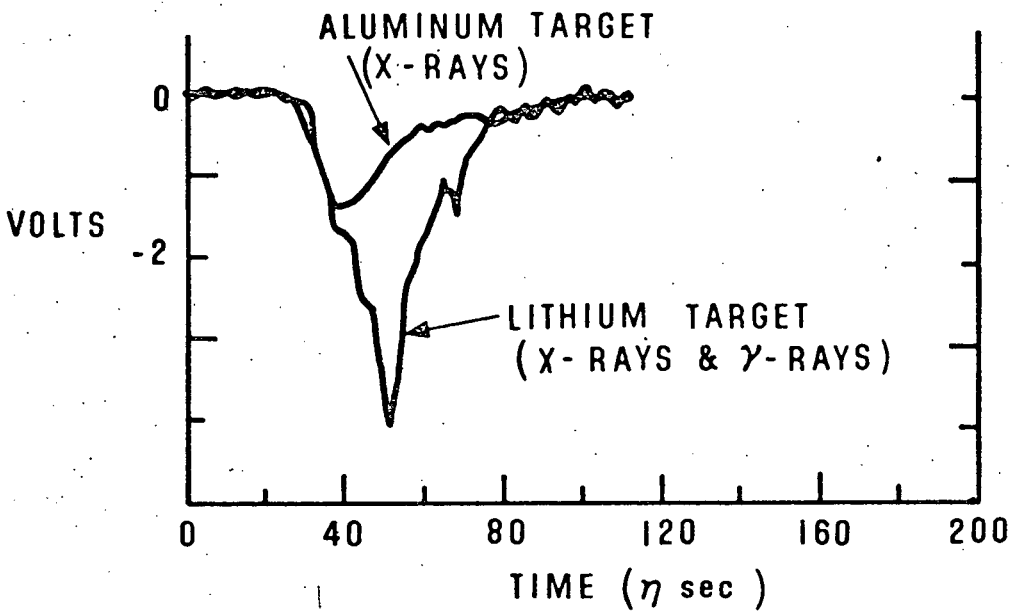
ALUMINUM TARGET
(X-RAYS)
0
VOLTS
-2
LITHIUM TARGET
(X-RAYS & γ-RAYS)
0
40
80
120
160
200
TIME (η sec)

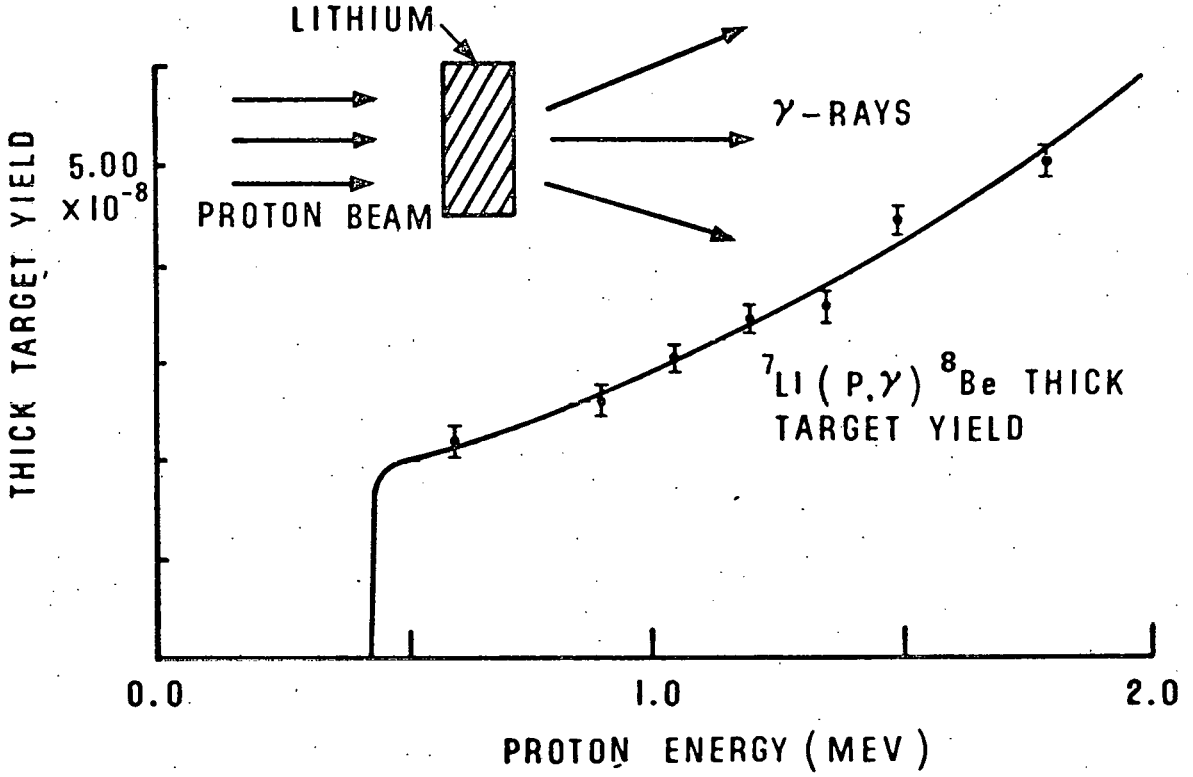
LITHIUM
γ-RAYS
PROTON BEAM
THICK TARGET YIELD
5.00
×10⁻⁸
⁷LI(P,γ)⁸Be THICK
TARGET YIELD
0.0
1.0
2.0
PROTON ENERGY (MEV)

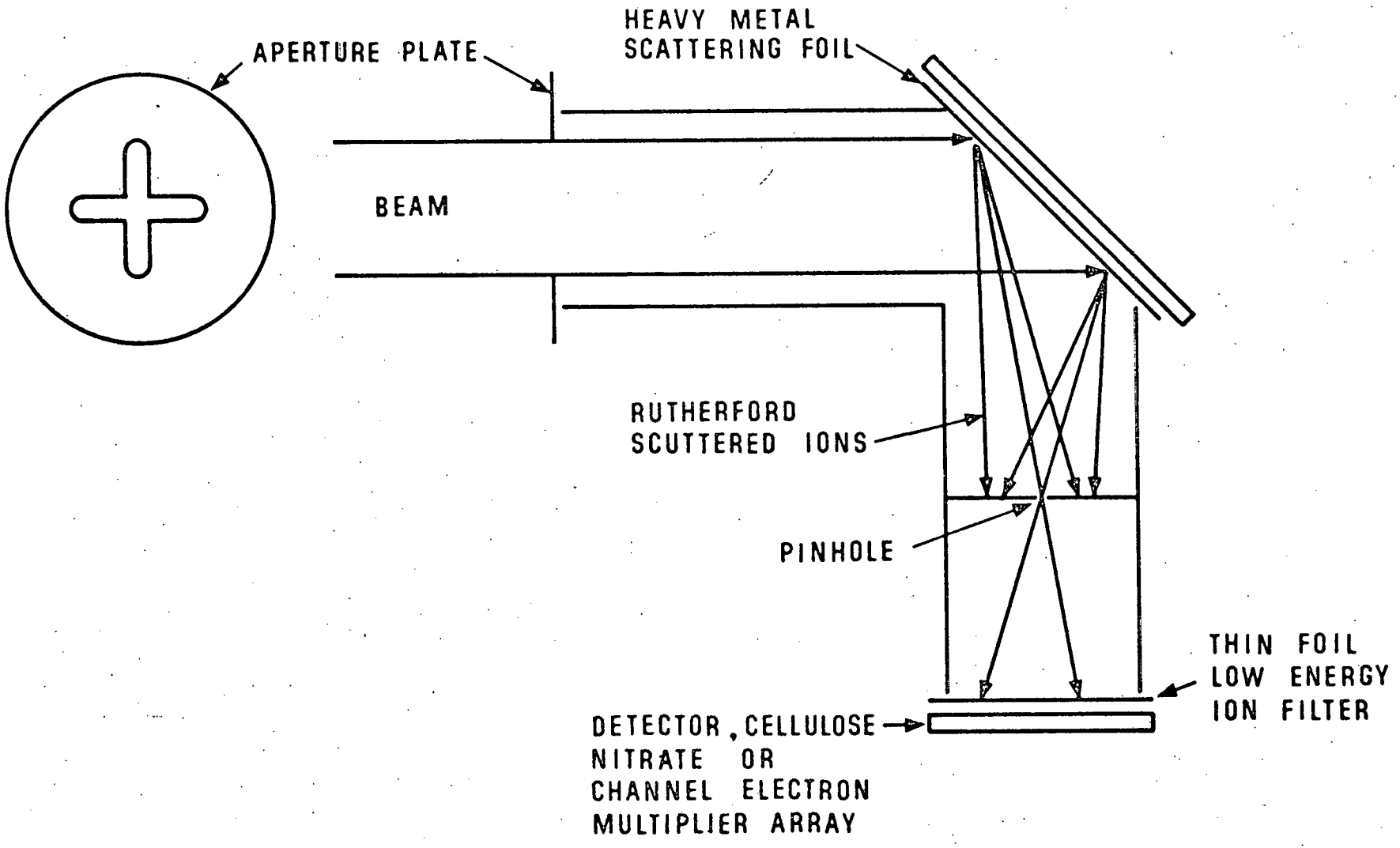
APERTURE PLATE
HEAVY METAL
SCATTERING FOIL
BEAM
RUTHERFORD
SCUTTERED IONS
PINHOLE
THIN FOIL
LOW ENERGY
ION FILTER
DETECTOR, CELLULOSE
NITRATE OR
CHANNEL ELECTRON
MULTIPLIER ARRAY

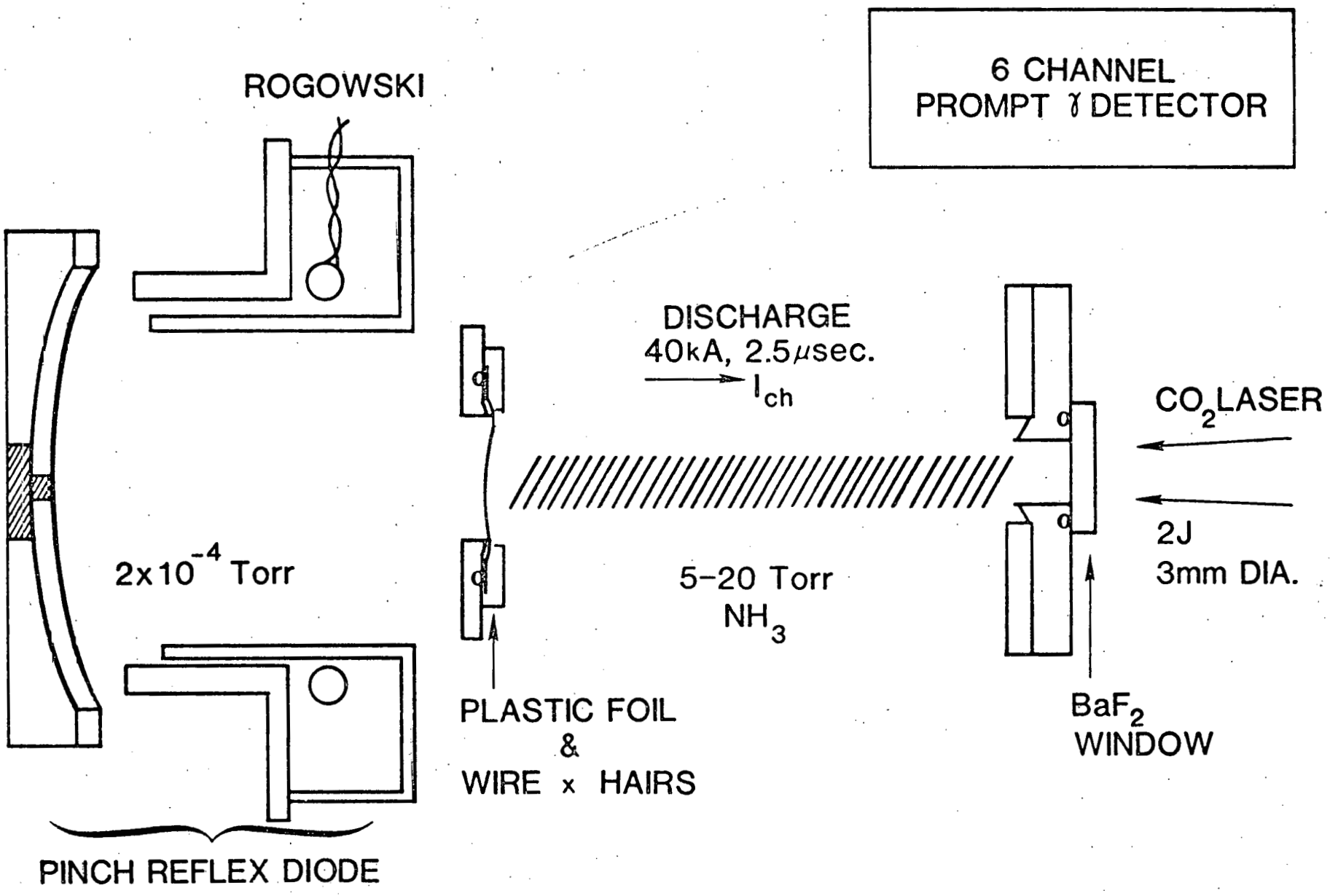
6 CHANNEL
PROMPT γ DETECTOR
ROGOWSKI
DISCHARGE
40kA, 2.5μsec.
I_{ch}
CO_2 LASER
2J
3mm DIA.
$2x10^{-4}$ Torr
5-20 Torr
NH_3
PLASTIC FOIL
&
WIRE x HAIRS
BaF_2
WINDOW
PINCH REFLEX DIODE

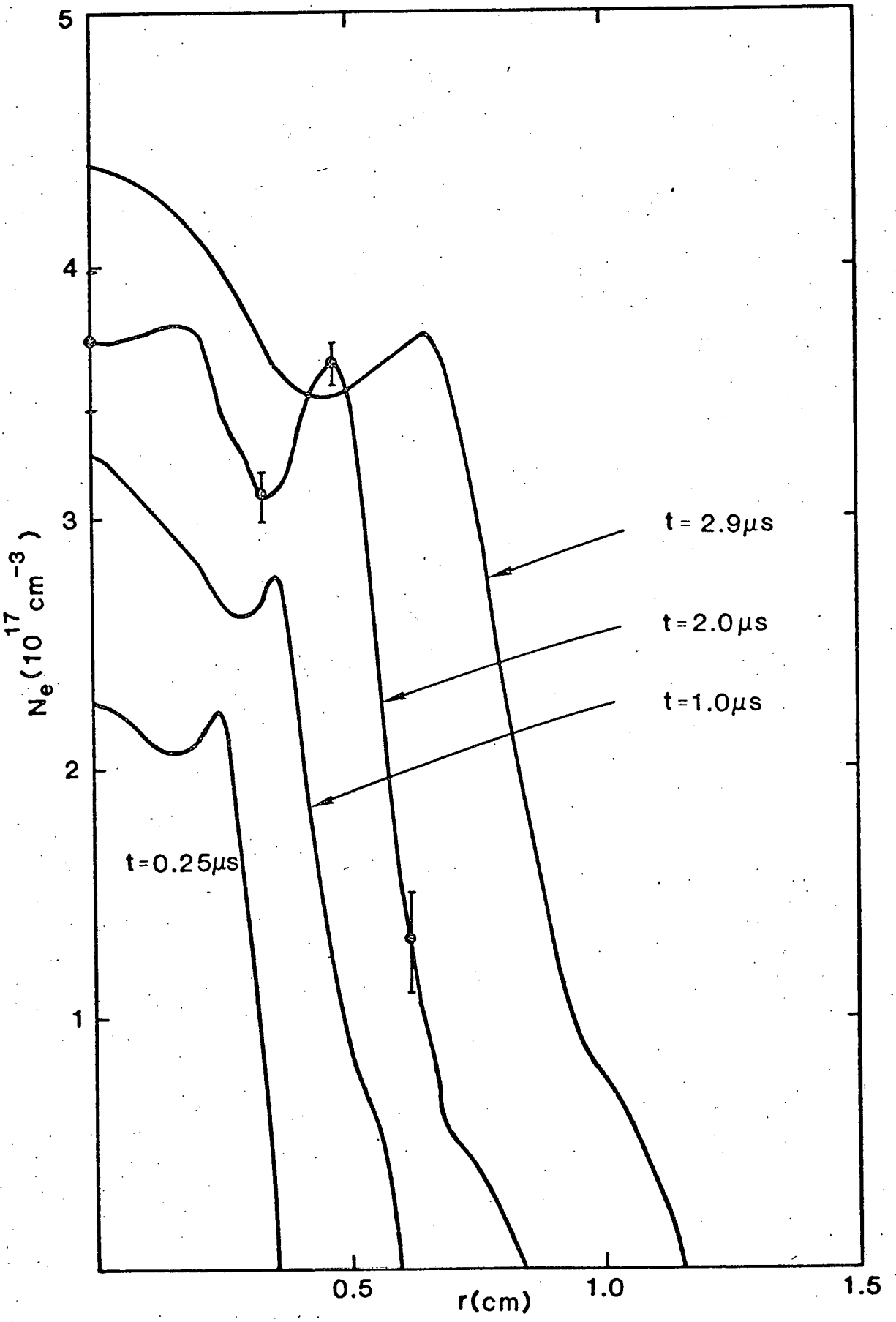
5
4
3
2
1
$N_e(10^{17}cm^{-3})$
t = 2.9μs
t = 2.0μs
t = 1.0μs
t = 0.25μs
0.5
1.0
1.5
r(cm)